March-April 2020
ISSN: 0193-4120 Page No. 2342 - 2353

Space Vector Technique for the Direct Three-Level Matrix Converter

M. Sivaramkrishnan[1] Dr. A. Amudha[2] Dr. M. Siva Ramkumar[3]
[1]Research Scholar, Dept of EEE, Karpagam Academy of Higher Education
[2]Prof and Head, Dept of EEE, Karpagam Academy of Higher Education
[3]Asst Prof, Dept of EEE, Karpagam Academy of Higher Education
krishbe95@gmail.com

Article Info
Volume 83
Page Number: 2342 - 2353
Publication Issue:
March - April 2020

Article History
Article Received*: 24 July 2019*
Revised*: 12 September 2019*
Accepted*: 15 February 2020*
Publication*: 19 March 2020*

Abstract:
The space vector PWM method for the immediate three-level grid converter has been proposed for orchestrating adjusted sinusoidal three-level yield voltages from adjusted and lopsided Non-sinusoidal information voltages. Moreover, conduction misfortunes and exchanging misfortunes were demonstrated for the DTMC and a relative investigation of the equivalent for the CMC and the DTMC has been completed. MATLAB recreation and equipment results confirm the adequacy of the proposed system. The THD of the yield voltage is lower for the DTMC when contrasted with the CMC. Be that as it may, the exchanging misfortunes for the DTMC are higher than those of the CMC.

1. INTRODUCTION

The voltage loads on the force devices can be diminished by using amazing inverters (MLIs) (Celanovic and Boroyevich 2000, Lopez et al 2008 and Aneesh et al 2009). MLIs award the use of lower rating power supplies and force contraptions for achieving a better return control rating. Using a comparative idea in the system converters, another gathering of converters called amazed grid converters progressed with different thoughts: I) Supplanting each bidirectional switch in the CMC with n cells, each telephone involving a capacitor related with the point of convergence of the H Extension (Erickson and Al-Naseem 2001 and Erickson et al 2006). This topology makes amazed yield anyway to the detriment of an undeniably tangled circuit course of action and parity method. ii) Altering the topology of the IMC with additional switches, which makes available two particular voltages, levels at the yield, i.e., the stage and the line voltages (Meng Yeong Lee et al 2010). This topology is practical for two-level and three-level voltage change with less frustrated circuit arrangement and guideline technique when diverged from (i). Modified IMC based three-level converter uses the diode caught stunned space vector framework (Meng Yeong Lee et al 2010) on the inverter side and the normal space vector procedure on the rectifier side In this part, another class of direct three-level network converter (DTMC) nearby its change strategies are made and its show is analyzed.

1.1 PROBLEM FORMULATION

The Objective of this part is to develop another DTMC topology to be explicit, the quick three-level network converter, which requires three bidirectional switches of lower assessments (arrange voltage evaluated) and the CMC topology. The structure is a 4 × 3 system converter that supports the development in the yield voltage levels by making the source unprejudiced access to the pile terminals. Despite the

March-April 2020
ISSN: 0193-4120 Page No. 2342 - 2353

stunning action, the converter in like manner can control the bi-directional force stream. The proposed DTMC is evaluated by proliferation and hardware experimentation. The equalization arrangement of the DTMC uses the amazing space vector balance technique nearby the proposed unbiased current modifying strategy. The identical is executed using the Xilinx based structure generator office, which is open as an instrument compartment in MATLAB R2010a, close by an FPGA.

1.3 PROPOSED TOPOLOGY

A DTMC in its ordinary structure showed up in Figure 1, includes three arms that are related to the source and one arm related to the star point (unprejudiced) of the data channel capacitances. Figure 1 depicts the general course of action of the proposed DTMC structure which contains a CMC and a neutral point connecter

1.3.1 Indirect Matrix Converter Representation for the DTMC

The proposed DTMC topology contains an assortment of 4 × 3 bidirectional switches, which consolidates the 3 × 3 switches of the CMC and three additional switches for making the unprejudiced reason for the information channel capacitance to be available at the store terminals. Conditions (5.1) and (5.2) give the yield voltages and the data streams of the DTMC.

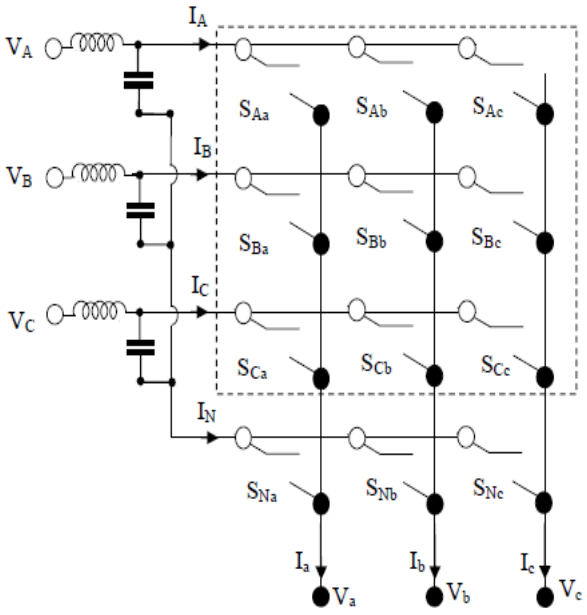

Figure 1 Topology of the direct three-level matrix converter

$$\begin{bmatrix} V_a \\ V_b \\ V_c \end{bmatrix} = \begin{bmatrix} S_{Aa} & S_{Ba} & S_{Ca} & S_{Na} \\ S_{Ab} & S_{Bb} & S_{Cb} & S_{Nb} \\ S_{Ac} & S_{Bc} & S_{Cc} & S_{Nc} \end{bmatrix} \times \begin{bmatrix} V_A \\ V_B \\ V_C \\ 0 \end{bmatrix}$$

$$\begin{bmatrix} I_A \\ I_B \\ I_C \\ I_N \end{bmatrix} = \begin{bmatrix} S_{Aa} & S_{Ab} & S_{Ac} \\ S_{Ba} & S_{Bb} & S_{Bc} \\ S_{Ca} & S_{Cb} & S_{Cc} \\ S_{Na} & S_{Nb} & S_{Nc} \end{bmatrix} \times \begin{bmatrix} I_a \\ I_b \\ I_c \end{bmatrix} \quad \ldots (1 \& 2)$$

Since the DTMC is given by a voltage source, the data stages ought to never be shorted, and on account of the inductive thought of the pile, the yield stages ought to never be left open. These impediments are recognized by Condition (3).

$$S_{Aj}+S_{Bj}+S_{Cj}+S_{Nj}=1 \qquad j\in\{a,b,c\} \quad \ldots(3)$$

The DTMC can be decoupled into a roaming three-level system converter (ITMC) involving a designed two-level converter (FTC – input converter) and a

March-April 2020
ISSN: 0193-4120 Page No. 2342 - 2353

nonexistent inverter (FI - yield converter), as showed up in Figure 2

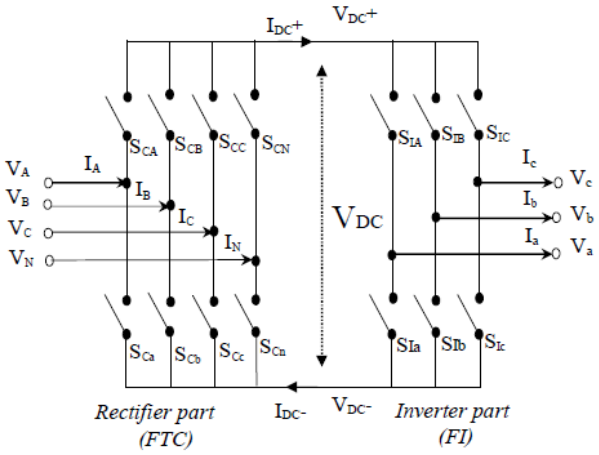

Figure 2 Topology of the indirect three-level matrix converter

The FTC contains three-phase arms and one unprejudiced arm. Turning ON any of the two-phase arms prompts the line voltage being open at the FDCB and turning ON any one phase arm with the fair arm prompts the stage voltage being available at the FDCB. This results in twelve powerful voltage vectors on the rectifier side. This decoupled depiction unravels the control of the data current and the yield voltage in DTMC, as delineated in the accompanying region.

1. Literature Survey

Insightful strong waste receptacle is fundamental to create and proficient and dynamic waste administration framework. This examination displays the usage and execution of an incorporated detecting framework and calculation for the strong waste receptacle to robotize the strong waste assortment process. A few detecting techniques have been incorporated and have joined their decisions that offer the discovery of container condition and its parameter estimation. Various trials have been led to evaluate the working of the model framework. The results demonstrated that the detecting framework with the calculation is effective and clever and can be essentially used to robotize any strong waste receptacle assortment process.

A few investigate has been done in the course of the most recent couple of decades concerning strong waste observing and the executives. In any case, a couple of them managed continuous canister status information with a thought process to actualize dynamic planning and directing methodology for a programmed strong waste assortment framework. The framework can catch the picture when the waste assortment vehicle came to the region of the container. As the control focus doesn't get the ongoing container status information, it relies upon the chronicled information for the assortment course. The analysts built up a container by utilizing a few kinds of sensors like a light-transmitting diode (LED), camera, ultrasonic, pressure and so forth for early identification of the receptacle status. Be that as it may, the framework can't react immediately when waste is tossed inside the canister. The creator reports the framework that has not adequate data about the receptacle level estimation systems and the dynamicity.

3. SPACE VECTOR MODULATION TECHNIQUE FOR THE DTMC

The exchanging capacity for the DTMC is spoken to as the result of the rectifier exchanging capacity and the inverter exchanging capacity and is given by

$$\begin{bmatrix} S_{Aa} & S_{Ba} & S_{Ca} & S_{Na} \\ S_{Ab} & S_{Bb} & S_{Cb} & S_{Nb} \\ S_{Ac} & S_{Bc} & S_{Cc} & S_{Nc} \end{bmatrix} = \begin{bmatrix} S_{IA} & S_{Ia} \\ S_{IB} & S_{Ib} \\ S_{IC} & S_{Ic} \end{bmatrix} \times \begin{bmatrix} S_{CA} & S_{CB} & S_{CC} & S_{CN} \\ S_{Ca} & S_{Cb} & S_{Cc} & S_{Cn} \end{bmatrix} \quad \ldots.(4)$$

The exchanging states for orchestrating the necessary flows and voltages are depicted in the accompanying subsections.

March-April 2020
ISSN: 0193-4120 Page No. 2342 - 2353

3.1 The Fictitious Two-Level Converter Stage

Tolerating that the yield of the FTC is a reliable current source IDC, the space vector for all genuine trading states is constrained by Conditions (5) to (7).

$$I_\alpha = I_A + I_B \cos\frac{2\pi}{3} + I_C \cos\frac{4\pi}{3}$$

$$I_\beta = I_B \sin\frac{2\pi}{3} + I_C \sin\frac{4\pi}{3}$$

$$I_0 = I_A + I_B + I_C$$

… (5, 6, 7)

As portrayed in Area 1.3.1, turning ON the unbiased arm makes the present stream in the sourcing fair realizing the space vector having a section along the I0 rotate. Table 1.1 gives the space vector parts for different real trading states and Figure 3(a) shows the space vectors course

Type	Vector	$\begin{bmatrix} S_{CA} & S_{CB} & S_{CC} & S_{CN} \\ S_{Ca} & S_{Cb} & S_{Cc} & S_{Cn} \end{bmatrix}$	I_A	I_B	I_C	$I_N=I_0$	I_{in}	$\angle I_{in}$	V_{DC}
Active long vectors	I_{L1}[AB]	$\begin{bmatrix}1000\\0100\end{bmatrix}$	$+I_{DC}$	$-I_{DC}$	0	0	$\sqrt{3}I_{DC}$	330^0	V_{AB}
	I_{L2}[AC]	$\begin{bmatrix}1000\\0010\end{bmatrix}$	$+I_{DC}$	0	$-I_{DC}$	0	$\sqrt{3}I_{DC}$	30^0	V_{AC}
	I_{L3}[BC]	$\begin{bmatrix}0010\\0001\end{bmatrix}$	0	$+I_{DC}$	$-I_{DC}$	0	$\sqrt{3}I_{DC}$	90^0	V_{BC}
	I_{L4}[BA]	$\begin{bmatrix}0100\\1000\end{bmatrix}$	$-I_{DC}$	$+I_{DC}$	0	0	$\sqrt{3}I_{DC}$	150^0	V_{BA}
	I_{L5}[CA]	$\begin{bmatrix}0010\\1000\end{bmatrix}$	$-I_{DC}$	0	$+I_{DC}$	0	$\sqrt{3}I_{DC}$	210^0	V_{CA}
	I_{L6}[CB]	$\begin{bmatrix}0010\\0100\end{bmatrix}$	0	$-I_{DC}$	$+I_{DC}$	0	$\sqrt{3}I_{DC}$	270^0	V_{CB}
Active short vectors	I_{P1}[AN]	$\begin{bmatrix}1000\\0001\end{bmatrix}$	$+I_{DC}$	0	0	$-I_{DC}$	I_{DC}	0^0	V_{AN}
	I_{P2}[NC]	$\begin{bmatrix}0001\\0010\end{bmatrix}$	0	0	$-I_{DC}$	$+I_{DC}$	I_{DC}	60^0	V_{NC}
	I_{P3}[BN]	$\begin{bmatrix}0100\\0001\end{bmatrix}$	0	$+I_{DC}$	0	$-I_{DC}$	I_{DC}	120^0	V_{BN}
	I_{P4}[NA]	$\begin{bmatrix}0001\\1000\end{bmatrix}$	$-I_{DC}$	0	0	$+I_{DC}$	I_{DC}	180^0	V_{NA}
	I_{P5}[CN]	$\begin{bmatrix}0010\\0001\end{bmatrix}$	0	0	$+I_{DC}$	$-I_{DC}$	I_{DC}	240^0	V_{CN}
	I_{P6}[NB]	$\begin{bmatrix}0001\\0100\end{bmatrix}$	0	$-I_{DC}$	0	$+I_{DC}$	I_{DC}	300^0	V_{NB}
Zero vectors	I_Z	$\begin{bmatrix}1&0&0&0\\1&0&0&0\end{bmatrix}\begin{bmatrix}0&1&0&0\\0&1&0&0\end{bmatrix}$ $\begin{bmatrix}0&0&1&0\\0&0&1&0\end{bmatrix}\begin{bmatrix}0&0&0&1\\0&0&0&1\end{bmatrix}$					0		0

where, $I_{in}=\sqrt{I_\alpha{}^2+I_\beta{}^2}$ and $\angle I_{in}=\tan^{-1}\frac{I_\beta}{I_\alpha}$.

Table 1.1 Space vectors for the fictitious two-level converter

Vectors spoke to by I (dynamic long vectors) are standard rectifier space vectors, which don't add to the objective current. Vectors addressed by IPi (dynamic short vectors) add to the fair current. To ensure that the data current is sinusoidal, the reference space vector must lie on the αβ plane requiring the impartial current to be zero on the use of the vector IPi. This is finished by applying also the adjacent IPi vector which lies on the upper and the lower portions of the αβ plane. This ensures the ordinary objective current is zero over a trading period. The model in Table 2 explains the equal

Switching time	Applied vectors	I_A	I_B	I_C	I_N	V_{DC}
$\frac{T_s}{2}$	I_{P6}	0	$-I_{DC}$	0	$+I_{DC}$	V_{NB}
$\frac{T_s}{2}$	I_{P1}	$+I_{DC}$	0	0	$-I_{DC}$	V_{AN}
T_s	$I_{VP1}=\frac{1}{2}I_{P6}+\frac{1}{2}I_{P1}$	$+\frac{1}{2}I_{DC}$	$-\frac{1}{2}I_{DC}$	0	0	$\frac{1}{2}V_{AB}$

Table 1.2 Neutral current balancing and virtual vector synthesis

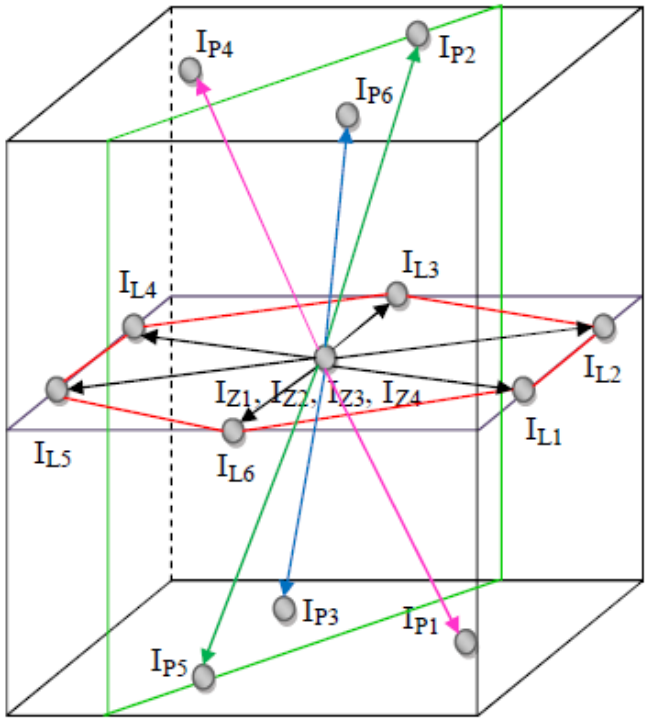

March-April 2020
ISSN: 0193-4120 Page No. 2342 - 2353

Figure 3(a) Space vectors of the FTC

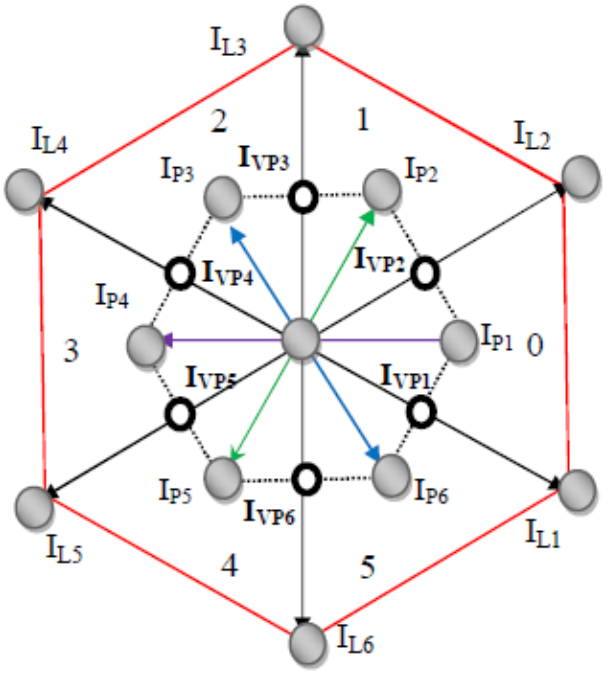

Figure 3(b) Space vectors and virtual vectors of the FTC

Virtual vectors	Sharing vectors	I_A	I_B	I_C	$I_N = I_0$	I_{in}	$\angle I_{in}$	V_{DC}
I_{VP1}[AN]	I_{P6},I_{P1}	$+\frac{1}{2}I_{DC}$	$-\frac{1}{2}I_{DC}$	0	0	$\frac{\sqrt{3}}{2}I_{DC}$	330^0	$\frac{1}{2}V_{AB}$
I_{VP2}[NC]	I_{P1},I_{P2}	$+\frac{1}{2}I_{DC}$	0	$-\frac{1}{2}I_{DC}$	0	$\frac{\sqrt{3}}{2}I_{DC}$	30^0	$\frac{1}{2}V_{AC}$
I_{VP3}[BN]	I_{P2},I_{P3}	0	$+\frac{1}{2}I_{DC}$	$-\frac{1}{2}I_{DC}$	0	$\frac{\sqrt{3}}{2}I_{DC}$	90^0	$\frac{1}{2}V_{BC}$
I_{VP4}[NA]	I_{P3},I_{P4}	$-\frac{1}{2}I_{DC}$	$+\frac{1}{2}I_{DC}$	0	0	$\frac{\sqrt{3}}{2}I_{DC}$	150^0	$\frac{1}{2}V_{BA}$
I_{VP5}[CN]	I_{P4},I_{P5}	$-\frac{1}{2}I_{DC}$	0	$+\frac{1}{2}I_{DC}$	0	$\frac{\sqrt{3}}{2}I_{DC}$	210^0	$\frac{1}{2}V_{CA}$
I_{VP6}[NB]	I_{P5},I_{P6}	0	$-\frac{1}{2}I_{DC}$	$+\frac{1}{2}I_{DC}$	0	$\frac{\sqrt{3}}{2}I_{DC}$	270^0	$\frac{1}{2}V_{CB}$

Table 1.3 Virtual current space vectors

Figure 4(a) shows section zero of the space vector outline of the FTC. Each division contains two unique long vectors, two powerful virtual short vectors, and four zero vectors. To incorporate the important reference input current and the FDCB voltage, the three nearest current vectors (Busquets-Monge et al 2004) are picked, as showed up in Figure 4(b), dependent upon the alteration record mc of the FTC.

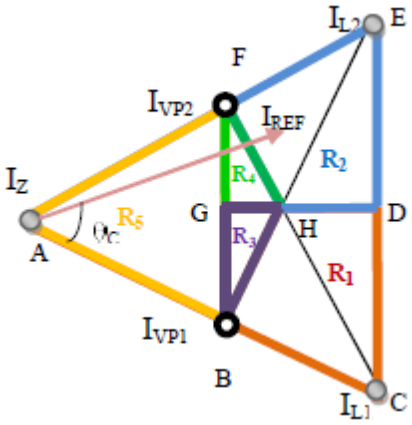

Figure 4(a) Sector region identification of the FTC

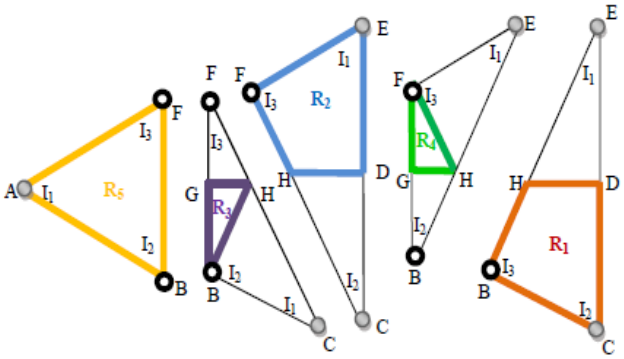

Figure 4(b) Region vector identification of the FTC

To perceive the territory wherein the reference vector lies, states of the three lines are induced and showed up in Figure 5 Table 1.4 gives the standards for recognizing the locale where the reference vector lies in the FTC for different estimations of equalization records mc.

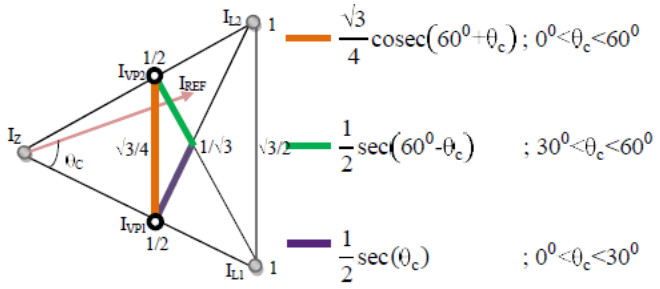

Figure 5 Equations of lines used for identifying regions in the FTC

March-April 2020
ISSN: 0193-4120 Page No. 2342 - 2353

Sl. No.	Region	Conditions
1	R_1	$m_c > \frac{1}{2}\sec(\theta_c)$; $0^0 < \theta_c < 30^0$
2	R_2	$m_c > \frac{1}{2}\sec(60^0-\theta_c)$; $30^0 < \theta_c < 60^0$
3	R_3	$\frac{\sqrt{3}}{4}\operatorname{cosec}(60^0+\theta_c) < m_c \leq \frac{1}{2}\sec(\theta_c)$; $0^0 < \theta_c < 30^0$
4	R_4	$\frac{\sqrt{3}}{4}\operatorname{cosec}(60^0+\theta_c) < m_c \leq \frac{1}{2}\sec(60^0-\theta_c)$; $30^0 < \theta_c < 60^0$
5	R_5	$m_c \leq \frac{\sqrt{3}}{4}\operatorname{cosec}(60^0+\theta_c)$; $0^0 < \theta_c < 60^0$

Table 4 Region identification for a given IREF

Obligation patterns of the picked vectors for different areas are prepared using Condition (8), where (xi, Yi) are the bearings of the picked vector Ii and di is its commitment cycle. X and Y are the bearings of the reference vector IREF and are given by Condition (9).

$$\begin{bmatrix} x_1 & x_2 & x_3 \\ y_1 & y_2 & y_3 \\ 1 & 1 & 1 \end{bmatrix} \begin{bmatrix} d_1 \\ d_2 \\ d_3 \end{bmatrix} = \begin{bmatrix} X \\ Y \\ 1 \end{bmatrix} \quad \ldots (8)$$

$$X = m_c \times \cos\theta_c \quad \& \quad Y = m_c \times \sin\theta_c \quad \ldots (9)$$

While enrolling in the commitment cycle, the part in Figure 6(a) is turned as showed up in Figure 6 (b). The bearings are picked by the locale wherein the reference vector lies, as showed up in Figure 6 (b). Table 5 gives the commitment cycles derived for different zones.

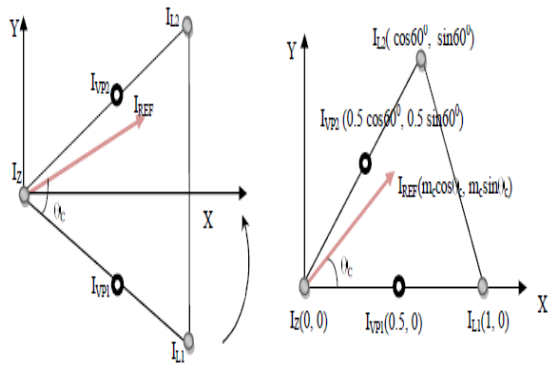

Figure 6 (a) Sector 1 and (b) sector 1 rotated

Region	Duty Cycle		
	d_1- I_1	d_2- I_2	d_3 - I_3
R_1	$\frac{2}{\sqrt{3}} m_c \sin(\theta_c)$	$2\, m_c \cos(\theta_c) - 1$	$2 - \frac{4}{\sqrt{3}} m_c \sin(60^0+\theta_c)$
R_2	$2\, m_c \sin(30^0+\theta_c) - 1$	$\frac{2}{\sqrt{3}} m_c \sin(60^0-\theta_c)$	$2 - \frac{4}{\sqrt{3}} m_c \sin(60^0+\theta_c)$
R_3	$\frac{4}{\sqrt{3}} m_c \sin(60^0+\theta_c) - 1$	$\frac{4}{\sqrt{3}} m_c \sin(60^0-\theta_c)$	$2 - 4\, m_c \cos(\theta_c)$
R_4	$\frac{4}{\sqrt{3}} m_c \sin(60^0+\theta_c) - 1$	$2 - 4\, m_c \sin(30^0+\theta_c)$	$\frac{4}{\sqrt{3}} m_c \sin\theta_c$
R_5	$1 - \frac{4}{\sqrt{3}} m_c \sin(60^0+\theta_c)$	$\frac{4}{\sqrt{3}} m_c \sin(60^0-\theta_c)$	$\frac{4}{\sqrt{3}} m_c \sin\theta_c$

Table 5 Duty cycles for different regions in a given sector

$$d'_\gamma = \frac{d_\gamma}{d_\gamma + d_\delta} \quad \& \quad d'_\delta = \frac{d_\delta}{d_\gamma + d_\delta} \quad \ldots (10)$$

$$V'_{OUT} = d'_\gamma V_\gamma + d'_\delta V_\delta = \frac{V_{OUT}}{d_\gamma + d_\delta} \quad \ldots (11)$$

$$m_c = \frac{\sqrt{3}}{2} m_{DTMC}(d_\gamma + d_\delta) \quad \ldots (12)$$

IV. IMPLEMENTATION

a) ATMEGA32A Microcontroller

The principle capacity of the CPU center is to guarantee the right program execution. The CPU should in this manner have the option to get to recollections, perform estimations, control peripherals, and handle interrupts. In request to boost execution and parallelism, the AVR utilizes Harvard design – with independent recollections and transports for program and information. Directions in the Program memory are executed with a solitary level pipelining. While one guidance is being executed, the following guidance is pre-gotten from the Program memory. This idea empowers guidelines to be executed in each clock cycle. The Program memory is In-System Reprogrammable Flash memory.

March-April 2020
ISSN: 0193-4120 Page No. 2342 - 2353

b)Weighing System

Right now installed controller which controls the segments interfaced with it. The controller will work to have a place with the code composed of the program memory. A Load cell is utilized to gauge the absolute amount of the waste dumped in the canister. A heap cell is normally an electronic gadget (transducer) that is utilized to change overpower into an electrical sign.

This transformation is aberrant and occurs in two phases. Through a mechanical course of action, the power being detected distorts a strain measure. The strain measure changes over the distortion (strain) to electrical signs. Ordinarily, a heap cell comprises four strain measures in a Wheatstone connect design, but at the same time is accessible with a couple of strain checks.

c)Sensing System

An ultrasonic sensor which used to gauge the separation inside the receptacle by setting off an ultrasonic wave. Then the activated wave is caught by an ultrasonic beneficiary. At that point, the separation could ascertain by the meantime contrast between activated heartbeat and get beat. At whatever point the container arrives at as far as possible it will be close through bulb driven by electric hand-off.

d)Heater Unit

The IR part of the Structure will utilize the view interference between IR transmitter and beneficiary to insinuate at whatever point a jug embedded into the container unit, at that point the radiator is put at the non-expendable territory of the Smart Bin, which will annihilate the plastic dump inside the canister.

e)Printing System

The reason for smaller than usual printer which associated with RS232 Protocol is utilized to pass on the message through receipt about the status of dump feed by the client. Right now Smart Bin framework would give some review focuses to support themselves for utilizing it.

f)Communication Module

At long last over-burden canister need to hint condition about cleaning to their relating office. The correspondence among canister and regarded group correspondence have done by the GSM module. The GSM module has associated with the sequential correspondence port of the controller and it sends SMS through it.

4. DTMC OPERATION UNDER ABNORMAL INPUT CONDITIONS

From Condition (5.14) it will, in general, be exhibited that inside a section, mc shows up at the apex once when(d + d) =1 and shows up at the base worth twice when (d =0) or (d =0), and this repeats for all the six divisions. Along these lines, the dynamic assortment of the mc presents a sixth symphonious part 6fi at the FDCB, as showed up in Figure 7 (a), where fi is the essential repeat of the data voltage.

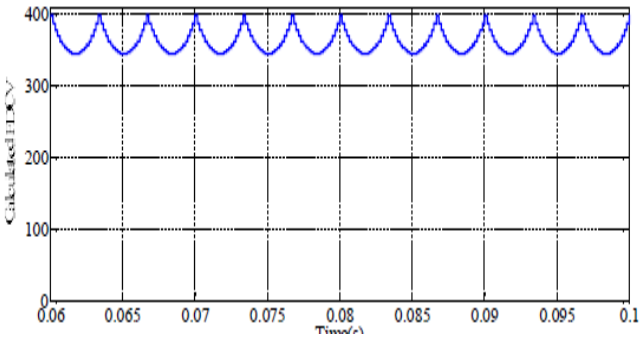

Figure 7 (a) Calculated FDCV with a balanced input voltage

March-April 2020
ISSN: 0193-4120 Page No. 2342 - 2353

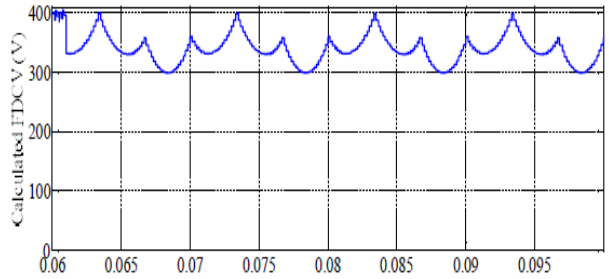

Figure 7 (b) Calculated FDCB voltages with an unbalanced input voltage

4. MODELING OF LOSSES IN THE CMC AND THE DTMC

There are three sorts of hardships in impact semiconductor devices to be explicit the ON, the of and the trading mishaps. The influence adversity in the device when it is "OFF" is irrelevant stood out from its impact incident when it is either "ON" or when it is encountering progress. The influence disaster in the device during its 'ON' state is known as the conduction setback while the impact hardships in the device during its change ('ON' to 'OFF' or a different way) known as the trading incident. Conduction hardship is the consequence of the voltage drop over the contraption and the current through the device when it is in the 'ON' state. A trading mishap is related to the aftereffect of blocking voltage and conduction current right now of trading; and if this is important, it is named as a hard trading disaster (Bierhoff and Fuchs 2004). If the trading happens when either the current through the device or the voltage over the contraption is right around zero, the substitution is insinuated as 'fragile trading' and the trading hardship in the device is unimportant. For an IGBT, there are two sorts of setbacks during hard trading: Ton_losses and Toff_losses, related to the device turn-ON and turn-OFF method independently. For a diode, the trading setback is realized by the switch recovery part that happens simply during the diode turn-OFF. Subsequently, the turn-ON setback for a diode isn't considered.

Switch transition	$S_1 \rightarrow S_2$	$S_2 \rightarrow S_1$	$S_1 \rightarrow S_2$	$S_2 \rightarrow S_1$
	$I_{out}+$		$I_{out}-$	
$V_{in}+$	E_{off}	$E_{on}+E_{rr\_D}$	$E_{on}+E_{rr\_D}$	E_{off}
$V_{in}-$	$E_{on}+E_{rr\_D}$	E_{off}	E_{off}	$E_{on}+E_{rr\_D}$

Table 6 Switching energy losses for switch S1 to switch S2 transition

From Table 6, it might be summarized that two substitution events, i.e., (I) first stage to second stage progress and (ii) second stage to at first stage change inside a trading cycle produces three trading mishaps to be explicit (I) an IGBT ON disaster, (ii) an IGBT OFF incident and (iii) a Diode OFF setback. Therefore, EswR = Age + Eoff + Err_D where Age and Eoff are the turning imperativeness for the IGBT ON and IGBT OFF switchings at the assessed VR and iR. Err_D is the DIODE OFF trading imperativeness at the assessed VR and iR. At the point when everything is said in done, for a particular advancement from the data arrange x to the information organize y, and the other route around the trading disaster is given by Condition (13).

$$E_{sw}(v_{xy}, i_L) = (E_{on} + E_{iff} + E_{rr\_D}) * (|v_{xy}| * i_L) / (V_R * i_R)$$

… (13)

From the Delay-Ic attributes of the datasheet, Ton, Toff, and Tr are recognized. Condition (14) gives the exchanging power misfortune.

$$S_{Losses}(v_{xy}, i_L) = \left(\frac{E_{on}}{T_{on}} + \frac{E_{off}}{T_{off}} + \frac{E_{rr\_D}}{T_r}\right) * (|v_{xy}| * i_L) / (V_R * i_R)$$

… (14)

4.1 Switching energy calculation for the CMC

Trading setbacks depend upon the alteration strategy. Right now, a twofold sided space vector trading strategy is picked for the CMC similarly as the DTMC. It might be seen that the improved trading method (Nielsen et al 1996) prompts eight reward events over all the three yield organizes in a trading

March-April 2020
ISSN: 0193-4120 Page No. 2342 - 2353

cycle Ts. Four of these reward events occur in a yield stage and two pay events each occur in the other two yield stages.

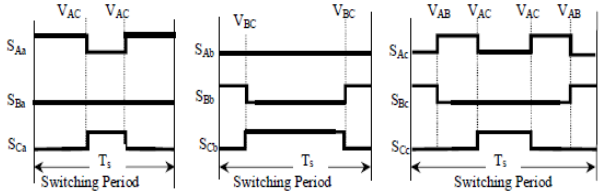

Figure 8 Commutation events of the CMC in a switching period for voltage sector 1 and current sector 1

4.2 Switching energy calculation for the DTMC

In the DTMC, two sorts of pay events happen explicitly: I) the line substitution where the blocking voltage is the line voltage and ii) the stage substitution where the blocking voltage is the stage voltage. Growing the streamlined distorted space vector switchings for the DTMC, as explained in Reference segment II, the amount of substitution events for a particular voltage section X and different locale of current part Y is resolved and given in Table 7

Commutation events	Converter sector - Y & Inverter sector -X				
	Regions of converter sector				
	R_1	R_2	R_3	R_4	R_5
Line voltage commutation	6	6	4/2	2/4	0
Phase voltage commutation	14	14	22	22	20

Table 7 Commutation events in a switching cycle Ts

5. SIMULATION

To assess the exhibition of the proposed topology with the changed space vector strategy, reenactment with R–L load was performed. Table 8 gives recreation parameters.

Quantity	Value
R-L Load	R = 20Ω , L = 21mH
Input phase voltage	100 V
Input voltage frequency	50 Hz
Input filter	L = 2 mH, C = 35 μF, R_d = 15 Ω
Output Voltage frequency	25 Hz
Switching frequency	6 kHz
Modulation Index	0.72, 0.5, 0.25

Table 8 Simulation parameters for the DTMC topology

For guideline records between and, the yield voltage switches between the dynamic long vectors and the dynamic short vectors yet for lower alteration records, the yield voltage switches between the dynamic short vectors and the zero vectors. Figure 5.11 shows the yield organize voltages, yield line voltages, input streams and yield streams for the voltage move extent that is changed from 0.72 to 0.5 at 0.4 s and 0.5 to 0.25 at 0.5 s. The consonant substance of the data and the yield streams increase with a decrease in the voltage move extent. In the CMC, the apex of the yield voltage is on numerous occasions the information voltage for all estimations of guideline records. Nevertheless, in the DTMC, the apex of the yield voltage is on different occasions the data voltage for the modification records more unmistakable than 34 while the zenith of the yield voltage is on various occasions the data voltage for balance documents lesser than 34. This prompts lower turning weight on the force devices because of the DTMC.

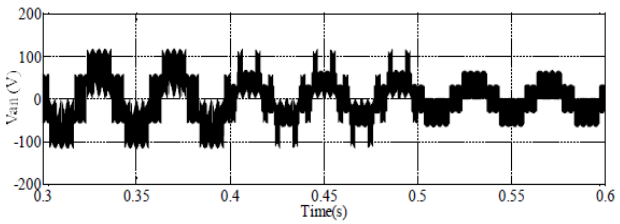

(a)

March-April 2020
ISSN: 0193-4120 Page No. 2342 - 2353

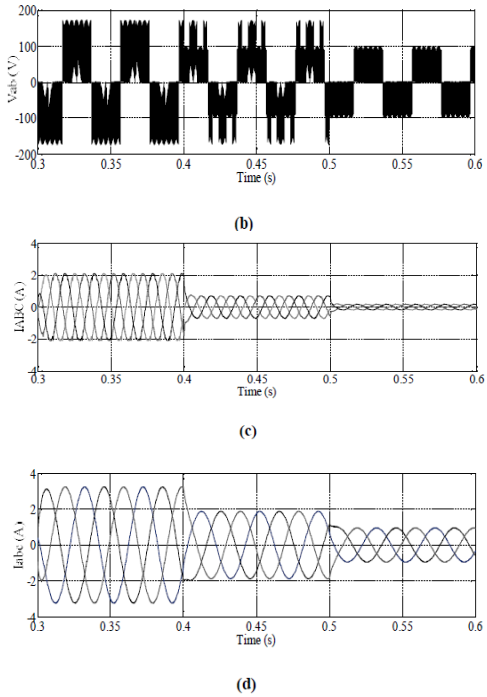

Figure 9 Performance of the DTMC with a balanced supply for different modulation indices (0.72, 0.5, and 0.25) (a) output phase voltage, (b) output line voltage, (c) input phase Current and (d) output phase current

A 20% unbalance in stage B was introduced. Additionally, second and third music with sizes of 4% and 7% of the major separately were added to all the three phases as showed up in Figure 10(a). By logically changing the change list, as explained in the past region, the effect of the unbalance and sounds has been mitigated in the yield voltages and streams, as showed up in Figures 10(b) and 10 (d). The unbalanced data streams are showed up in Figure 10(c).

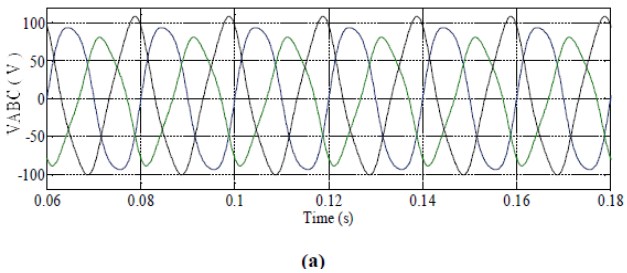

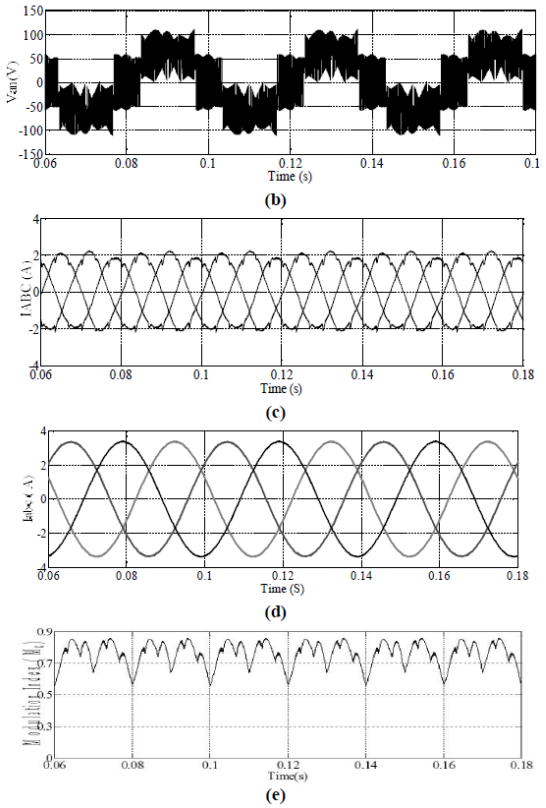

Figure 10 Performance of the DTMC with an unbalanced supply (a) output phase voltage, (b) output line voltage, (c) input phase current and (d) output phase current and (e) Modulation index

Conclusion

This task introduced simpler techniques for actualizing complex exchanging methodologies, considering and relieving the impacts of unbalance, and topological changes to build the exhibition lists. Additionally proposes tweak strategies to dispose of the normal mode voltage and another immediate torque control strategy for controlling an enlistment engine encouraged by the changed grid converter topology. In all cases, the course of the examination work is to concentrate on the improvement and investigation of the PWM systems for various control goals. In such a manner, a PWM control calculation has been built up that offers an exchanging system, named as the Base Mistake Exchanging Procedure (Wreckage), appropriate for framework converters

March-April 2020
ISSN: 0193-4120 Page No. 2342 - 2353

working under high exchanging frequencies. Its predominance lies in the simplicity of usage, straightforwardness, diminished exchanging misfortunes and its reasonableness at high exchanging frequencies. The work additionally presents a straightforward bearer based regulation procedure, named as the DIDC PWM strategy, as an elective method for actualizing the space vector system for the network converter. Given the examination did on the first DIDC PWM system, the theory proposes a changed control calculation

References

[1]. Nemoto, S. (2001). U.S. Patent No. 6,211,651. Washington, DC: U.S. Patent and Trademark Office.

[2]. C hiu, H. J., & Lin, L. W. (2006). Abidirectional DC–DC converter for fuel cell electric vehicle driving system. IEEE Transactions on Power Electronics, 21(4), 950-958.

[3]. Hu G H, Xu J M, Zhou J, and Hu X, "Design of Li-ion battery management system based on Atmega16," in Information Technology Applications in Industry, Zhang Wang Z J, Zhu S R, and Meng, Eds X M, vol. 1-42013, pp. 335–338, 2012.

[4]. Almeida, "Evaluation of the benefits of the introduction of electricity powered vehicles in an island," Energy Conversion and Management, vol. 76, pp. 541– 553, 2013.

[5]. Gao B, Zhang W, Tang Y, Hu M, Zhu M, and Zhan H, "Game theoretic energy management for residential users with dischargeable plug- in electric vehicles," Energies, vol. 7, no. 11, pp. 7499–7518, 2014.

[6]. Yang Y P and Jiang J M, "Optimal design of an axial-flux permanent magnet middle motor integrated in a cycloidal reducer for a pedal electric cycle," Energies, vol. 8, no. 12, pp. 14151–14167, 2015.

[7]. Jones T, Harms L, and Heine E, "Motives, perceptions and experiences of electric bicycle owners and implications for health, wellbeing and mobility," Journal of Transport Geography, vol. 53, pp. 41–49, 2016.

[8]. Dr. Siva Ganesh Malala, MIEEE, JayadeepuDadi and PavankumarDadi," Solar- Hydrogen Energy based Hybrid Electric Vehicle", 978-1-5386-1887-5/17 ©2017 IEEE.

[9]. Pindoriya R M, Student Member, IEEE, Rajpurohit B S, Senior Member, IEEE, Kumar R and Srivastava K N," Comparative Analysis of Permanent Magnet Motors and Switched Reluctance Motors Capabilities for Electric and Hybrid Electric Vehicles", 978-1-5386- 1138-8/18 ©2018 IEEE.

[10]. N. Eswaramoorthy, Dr.M. Siva Ramkumar, G. Emayavaramban, A. Amudha, S. Divyapriya, M. Sivaram Krishnan, D. Kavitha "A Control Strategy for A Variable Speed Wind Turbine with A Permanent Magnet Synchronous Generator Using Matrix Converter with SVPWM" International Journal of Recent Technology and Engineering, 8(1S4) pp 178-186

[11]. P. Jeyalakshmi, Dr.M. Siva Ramkumar, IR.V. Mansoor, A. Amudha, G. Emayavaramban, D. Kavitha, M. Sivaram Krishnan, "Application of Frequency based Matrix Converter in Wind Energy Conversion System Employing Synchronous Generator Using SVPWM Method" International Journal of Recent Technology and Engineering, 8(1S4) pp 187-195

[12]. Charles Stephen, .A. Amudha, K. Balachander, .Dr.M. Siva Ramkumar, G. Emayavaramban, IR.V. Manoor, "Direct Torque Control of Induction Motor Using SVM Techniques" International Journal of Recent Technology and Engineering, 8(1S5) pp 196-202

[13]. N. Saravanakumar, A. Amudha, G. Emayavaramban, Dr.M. Siva Ramkumar, S. Divyapriya, "Stability Analysis of Grid Integration of Photovoltaic Systems Using Partial Power Converters" International Journal of Recent Technology and Engineering, 8(1S5) pp 203-210

[14]. S.Divyapriya, K.T.Chandrasekaran, A.Amudha, Dr.M.Siva Ramkumar, G.Emayavaramban, "Low Cost Residential Micro Grid System based Home to Grid Backup Power Management" International

March-April 2020
ISSN: 0193-4120 Page No. 2342 - 2353

Journal of Recent Technology and Engineering, 8(1S5) pp 303-307

[15]. N. Thiyaagarajan, Dr.M. Siva Ramkumar, A. Amudha, G. Emayavaramban, M. Sivaram Krishnan, D. Kavitha, "SVPWM based Control of SCIG-Matrix Converter for Wind Energy Power Conversion System" International Journal of Recent Technology and Engineering, 8(1S5) pp 211-218

[16]. N. Seethalakshmi, A. Amudha, S. Divyapriya, G. Emayavaramban, Dr.M. Siva Ramkumar, IR.V. Mohamed Mansoo, "Voltage Frequency Controller with Hybrid Energy Storage System for PMSG Based Wind Energy Conversion System" International Journal of Recent Technology and Engineering, 8(1S5) pp 219-229

[17]. G. Suresh, A.Amudha, Dr.M. Siva Ramkumar,G. Emayavaramban, IR.V.Manoor, "Bidding Strategy of Electricity Market Considering Network Constraint in New Electricity Improvement Environment" International Journal of Recent Technology and Engineering, 8(1S5) pp 230-234

[18]. G. Krishnan, M. Siva Ramkumar, A. Amudha, G. Emayavaramban,S. Divyapriya, D. Kavitha, M. Sivaram Krishnan, "Control of A Doubly Fed Induction Generator for Wind Energy Conversion System Using Matrix Converter with SVPWM Technique" International Journal of Recent Technology and Engineering, 8(1S5) pp 235-243

[19]. S. Viswalingam, G. Emayavaramban, Dr.M. Siva Ramkumar, A. Amudha, K. Balachander, S. Divyapriya, IR.V. Mohamed Mansoor "Performance Analysis of a Grid Connected PV-Wind with Super Capacitor Hybrid Energy Generation & Storage System" International Journal of Recent Technology and Engineering, 8(1S5) pp 658-666

[20]. N.Pandiarajan, G.Emayavaramban, A.Amudha, Dr.M.Siva Ramkumar, IR.V.Mohamed Mansoor, K.Balachander, S.Divyapriya, M..Sivaram Krishnan, "Design and Electric Spring for Power Quality Improvement in PV-Based Dc Grid" International Journal of Recent Technology and Engineering, 8(1S5) pp 242-245

[21]. V.Jayaprakash, S.Divyapriya, A.Amudha, G.Emayavaramban,Dr.M.Siva Ramkumar, "Nano - Grid Smart Home With Plug-in Electric Vechicle using a Hybrid Solar-Battery Power Source" International Journal of Recent Technology and Engineering, 8(1S5) pp 246-248

[22]. K.T.Chandrasekaran, S.Divyapriya, A.amudha, Dr.M.Siva Ramkumar, G.Emayavaramban, "Modeling and Control of Micro Grid Based Low Price Residential Home to Grid Power Management System" International Journal of Recent Technology and Engineering, 8(1S5) pp 261-265

[23]. Dr.A.Amudha, M.Siva Ramkumar, M.Sivaram Krishnan "DESIGN AND SIMULATION OF ZETA CONVERTER WITH ZVZCS SWITCHING TECHNIQUE" Journal of Engineering and Applied Sciences ,14(9) pp 2764-2774 DOI: 10.3923/jeasci.2019.2764.2774

[24]. M. Sivaram Krishnan, S. Sri Ragavi, M. Siva RamKumar, D. Kavitha "Smart Asthma Prediction System using Internet of Things" Indian Journal of Public Health Research & Development, 10 (2) , pp 1103-1107 DOI:10.5958/0976-5506.2019.00445.5